

Temperature dependence of Lévy-type stick-slip diffusion of a gold nanocluster on graphite

Yutaka Maruyama

National Institute of Advanced Industrial Science and Technology (AIST), 2266-98 Anagahora, Shimo-shidami, Moriyama-ku, Nagoya 463-8560, Japan

(Received 1 October 2003; revised manuscript received 12 December 2003; published 22 June 2004)

In this paper we present results from a molecular dynamics study on the temperature dependence of Lévy-type stick-slip diffusion of a gold nanocluster (Au_{245}) on graphite. Exponents that characterize the power-law correlated diffusion dynamics are not universal, but vary with temperature. Although the diffusion dynamics conflicts with the usual equilibrium Arrhenius jump rate process, diffusion coefficients computed obey an Arrhenius law.

DOI: 10.1103/PhysRevB.69.245408

PACS number(s): 36.40.Sx, 05.40.Fb, 82.20.Db

I. INTRODUCTION

Surface diffusion of adsorbates in particular with many internal degrees of freedom has been intensely studied over the past few years.¹⁻³ This is because they interact with surfaces via qualitatively different potential energy from that for single adatoms and often exhibit novel complex behavior such as extremely large diffusivity (prefactors) and long jumps.

One of the most interesting findings is that the experimentally observed fast surface diffusion of gold nanoclusters on graphite¹ is probably a “Lévy-walk”^{4,5} or, more strictly, a “truncated Lévy-walk.”^{6,7} In the diffusion found with molecular dynamics (MD) simulations,^{5,7} sticking durations (periods of time which a gold cluster as a whole spends in oscillating before escaping from a potential well) and jump durations (periods of time between two successive stickings) both obey power-law distributions. Namely, long-lived long jumps and short stickings occur very frequently.

Frequent short stickings as well as frequent long-lived long jumps imply that the cluster is not always well thermalized within a potential well, conflicting with the picture of equilibrium Arrhenius jump rate processes,⁸ where jump and sticking durations are usually very short and long, respectively, and separable in time scale, and jumps that require an energy E occur, at least except for very high temperatures, in proportion to $\sim \exp(-E/k_B T)$ (k_B is Boltzmann’s constant). However, the experiments¹ have shown that the temperature dependence of diffusivity for the cluster surface diffusion is an Arrhenius-type activated one, which confuses us.

My question is whether the power-law correlated activation-relaxation (stick-slip) dynamics can be actually consistent with Arrhenius behavior? Computationally, temperature dependence of the power-law diffusion dynamics as well as that of diffusion coefficients has not been examined yet. This is because the absence of characteristic time scales makes the convergence of diffusivities and statistics remarkably slow, requiring extremely long ($> \mu\text{s}$) MD runs.⁷ Here I therefore study the temperature dependence in the wide temperature range of 200–670 K by performing extremely long (10 μs) MD simulations with a Langevin-thermostated two-dimensional (2-D) Frenkel–Kontrova (FK)-type⁹ cluster-surface model.⁷

We will see in the following that the power-law nature is in itself fairly robust to temperature change, but the exponents of the power-law distributions vary with temperature, i.e., they are not universal. In contrast to the usual surface diffusion, in which jumps are almost limited to adjacent sites, the ratio of long jumps increases significantly with temperature. Although the diffusion dynamics conflicts with the usual activation process, diffusion coefficients computed obey an Arrhenius law.

II. MODEL

Before constructing the model, two things are noted.

A first thing is that Lévy-type diffusion dynamics has been observed for both a dynamic graphite surface and a static one.⁵ This is probably due to the large difference in mass (or in vibration frequency) between gold and carbon atoms and the weak cluster–surface interaction, implying the applicability of a so-called “adiabatic elimination” of carbon’s fast degrees of freedom.

The second thing is the presence of power-law nature in the diffusion dynamics.^{5,7} As is well known for critical phase transitions¹⁰ and self-organized critical phenomena,¹¹ power-law nature, which arises in a system where many spatiotemporal length scales are important, is insensitive to the details of the system, such as the interaction between atoms or subsystems. Namely, the detailed and realistic engineering-type modeling of a power-law correlated system can be often needless, at least, to understand the global (long time) behavior of the system.

In accordance with the two things, the following simplified Langevin-thermostated 2-D FK-type⁹ cluster–surface model is adopted, which allows us to perform statistically sufficiently long ($> \mu\text{s}$) simulations very easily without losing essential physics, as demonstrated in Ref. 7.

The model cluster, illustrated in the upper left-hand inset of Fig. 1, is a three-dimensional crystalline gold cluster, Au_{245} , whose lowermost 37 atoms form a compact hexagon. (The size of the model cluster is close to that of Au_{250} clusters deposited in the experiments.¹) Au–Au interactions are

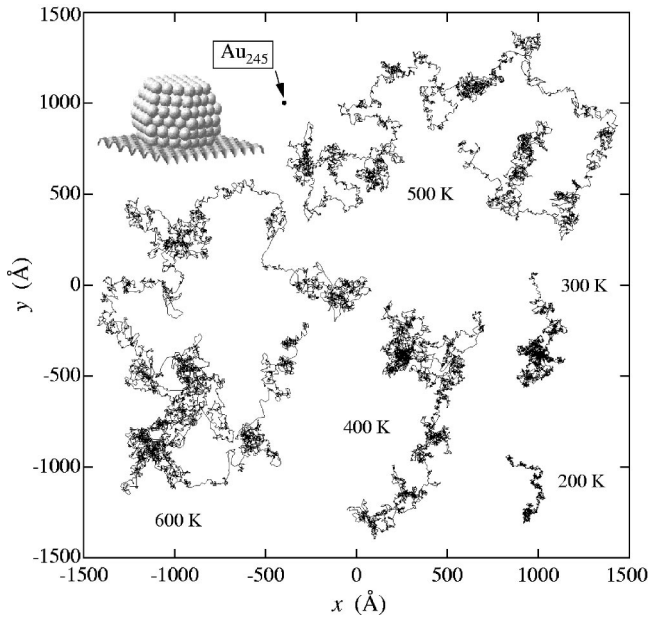


FIG. 1. $2 \mu\text{s}$ x - y trajectories of the clusters center of mass position for $T=200, 300, 400, 500,$ and 600 K. Upper left-hand inset: Snapshot of the gold nanocluster (Au_{245}) on graphite (v_{atom}). The diameter of the cluster is about 20 \AA , expressed as the small dot indicated by the arrow.

described by a Lennard-Jones (LJ) (6-12) potential and restricted to first nearest neighbors. This is based upon the principle of adoption of as simple a model as possible without losing the characteristic power-law stick-slip diffusion mechanism. The well depth of the LJ potential is set at 0.609 eV , which was derived from the bulk modulus and interatomic distance of bulk gold.

The LJ potential may be improper to investigate several features of a gold nanocrystal quantitatively, but can be employed to investigate the characteristic power-law correlated stick-slip diffusion dynamics in the temperature range of $200\text{--}670 \text{ K}$ sufficiently below the melting point of bulk gold 1337 K . (I confirmed that diffusion dynamics does not change very much even if a harmonic potential with the same bulk modulus is used.)

As shown in Ref. 5, a static graphite surface can represent the greater part of a dynamical graphite surface. However, the use of a static surface is inappropriate to investigate temperature dependence because it does not entirely enable us to take account of the thermalization effect according to temperature. Hence, here I use the following static potential surface with Langevin-thermostats.

On graphite surfaces, β -sites, which have no carbon atoms sitting beneath them in the adjoining graphite sheet, are preferential adsorption sites for metal adatoms.¹² The static potential surface, v_{atom} , is therefore defined not on the honeycomb lattice of graphite but on a triangular lattice with the lattice constant of graphite, a . (α -sites are omitted.) Here in this work, I express the potential surface by the three shortest wave vectors' terms of a 2-D Fourier series:

$$v_{\text{atom}}(x, y) = -\frac{2}{9}E_0 \left(\cos \left\{ \frac{2\pi}{a} \left[x + \frac{y}{\sqrt{3}} \right] \right\} + \cos \left\{ \frac{4\pi y}{\sqrt{3}a} \right\} + \cos \left\{ \frac{2\pi}{a} \left[x - \frac{y}{\sqrt{3}} \right] \right\} \right).$$

The amplitude of potential corrugation, E_0 , is set at 0.06 eV because it is thought to be a mere fraction of the binding energy of 0.26 eV/atom for large Au islands on graphite.¹² Since the interaction between gold clusters and graphite surfaces is weak, the relaxation of the graphite lattice in the presence of clusters is not taken into account. The Langevin-thermostats for the lowermost 36 atoms are described in terms of the under-damped Langevin dynamics,¹³ which enables us to introduce temperature into the static potential surface.

According to Ref. 5, there is a correlation between sticking states and changes of the z -coordinate of the cluster's center of mass; however, the changes are no more than 0.03 \AA at 500 K , which is only a twentieth part of the length scale ($\sim 0.6 \text{ \AA}$) of the x - y sticking motion of the cluster as a whole. Furthermore, the time scale (up to a few ns) of the changes is much larger than that ($\sim 20 \text{ ps}$) of the x - y sticking motion. These significant differences in spatiotemporal scales imply that the effect of the z -component of motion on the surface diffusion dynamics of the cluster as a whole is unimportant and separable from that of the x and y components. Hence, in accordance with the above principle, z -component variance in potential is not taken into account, and all the z interatomic distances of the cluster are always fixed.

The simplified model exhibits characteristic power-law correlated stick-slip diffusion dynamics, as shown in Ref. 7, and meets the purpose. Strictly speaking, however, a possibility that the suppression of the z -component invisibly causes differences between computational and experimental observations is not completely nil. As shown by Zhdanov,¹⁴ motions along and perpendicular to a surface can be inseparable for single atom surface diffusion. The presence of effects of the z -component on the diffusion dynamics and difference in the way the cluster and single atoms interact with surfaces are worthy of further study.

The dynamics of every atom except the lowermost Langevin-thermostatted 37 atoms is performed with the Verlet algorithm. The time step is 5 fs , and the Langevin damping-time constant is set to 100 ps .⁷

III. RESULTS AND DISCUSSION

I performed MD simulations of $10 \mu\text{s}$ for various temperatures in the range of $200\text{--}670 \text{ K}$. Figure 1 shows parts of x - y trajectories ($2 \mu\text{s}$) for $200, 300, 400, 500,$ and 600 K . Although we cannot clearly see from these trajectories, the cluster repeats stick-slip motion many times. In contrast to the usual adatom diffusion, jump durations can be longer than sticking durations, and the cluster diffusion proceeds mainly by long-lived long jumps which have no apparent influence of the lattice of the substrate. Sticking and jumps are both often accompanied by nearly free or oscillatory ro-

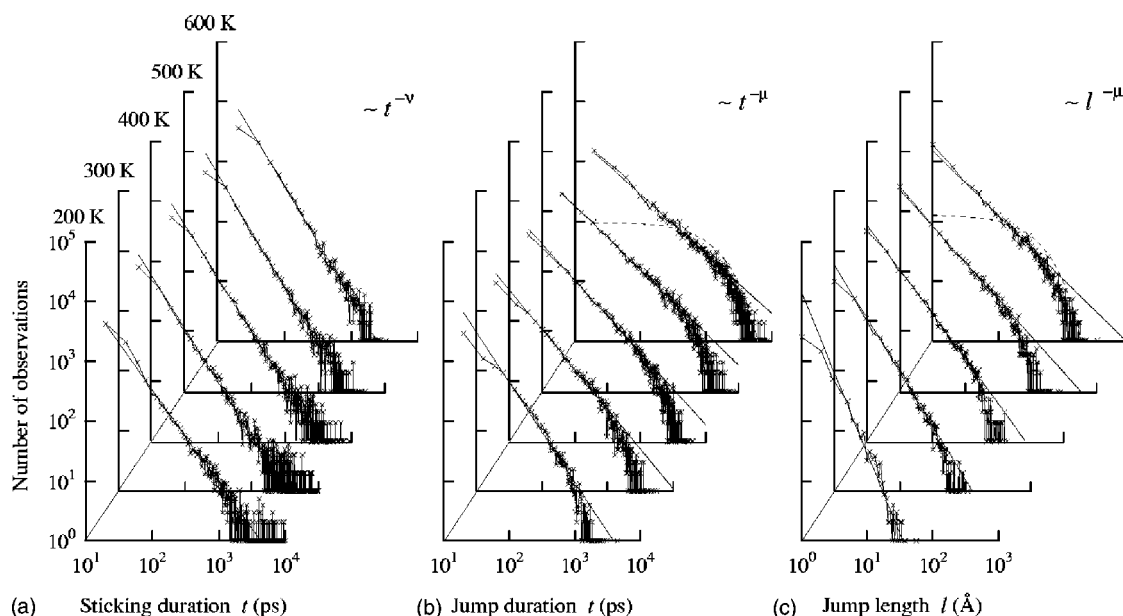


FIG. 2. Log–log plots of histograms of (a) sticking duration, (b) jump duration, and (c) jump length for $T=200, 300, 400, 500,$ and 600 K. The data were obtained from $10 \mu\text{s}$ MD simulations. Duration and length histogram bin widths are 20 ps and 1 \AA , respectively. The broken lines in (b) and (c) show exponential functions that are least-square-fitted to log–linear scaled data at 600 K. It can be clearly seen that the exponential functions do not fit well to the data, in particular, for short durations and lengths.

tations of the cluster as a whole. (More details of the diffusion dynamics have been described in the previous works.^{5,7})

From a cursory visual inspection of the trajectories, we can see that each trajectory consists of many length scales and has a characteristic of Lévy-walk,⁴ and that the ratio of long jumps increases significantly with temperature. To confirm this visual inspection statistically, all jumps and stickings in each x - y trajectory are distinguished in much the same way as Ref. 5: distance $d(t_i) = |\mathbf{R}(t_i - \tau_c/2) - \mathbf{R}(t_i + \tau_c/2)|$ is examined every 2 ps, and when $d(t_i) < d_c$ time t_i is classified as a sticking period. Here $\tau_c = 20$ ps is the period of sticking oscillation, which has no significant temperature dependence as shown later in Fig. 4(b), and $d_c = 0.6 \text{ \AA}$.

Jump durations are given as the intervals between two consecutive sticking durations. In the present work, to avoid the ambiguity between short stickings and jumps, I reclassified short sticking durations below τ_c as jump periods. Each jump length, l , is given as the distance between two consecutive sticking points.

Figure 2 shows log–log plots of histograms of (a) sticking durations, (b) jump durations, and (c) jump lengths for $T = 200, 300, 400, 500,$ and 600 K, which were obtained from $10 \mu\text{s}$ MD simulations. A first point to observe is that for each temperature the three histograms exhibit a power-law nature. We can see from Fig. 2(a) that sticking durations clearly obey a power-law distribution $\sim t^{-\nu}$ over almost two decades ($\sim 10^1 - 10^3$ ps). From Figs. 2(b) and 2(c), we can see that, except for the drop-off (the truncation of power-law tails^{6,7}) at large scales, jump durations and jump lengths both follow power-law distributions, $\sim t^{-\mu}$ and $\sim l^{-\mu'}$, respectively. The power-law nature, in particular, of the jump length distribution indicates that all the trajectories in Fig. 1 basically do share a characteristic of a Lévy-walk⁴ which has no typical jump length scale, as indicated in the cursory vi-

sual inspection of them. The drop-off (truncation) at large scales represents a transition from power-law decay to much faster (exponential) decay, meaning the suppression of infinitely long jumps. This suppression, which is presumably deeply related to both nonlinearity inherent in the diffusion dynamics and thermalization with surroundings, is unavoidable.

A second point to observe is that the power-law nature, which in itself is robust to temperature change, varies with temperature. We can find that truncation time and truncation length both increase with temperature (from 2 to 7 ns and from 30 to 100 \AA , respectively), while maximum sticking duration decreases (from 20 to 2 ns). In addition, we can find that the power-law exponents, ν , μ , and μ' , defined as the slopes of the sticking duration, jump duration, and jump length distributions, respectively, are not universal, but vary with temperature.

Figure 3(a) shows the temperature dependence of the exponents. We can see that μ and μ' both decrease with temperature, while ν increases: for μ from 1.55 to 0.96 , for μ' from 2.23 to 1.09 , and for ν from 1.58 to 1.91 . The decrease, in particular, in μ' represents an increase in the ratio of long jumps, proving the validity of the cursory visual inspection of the trajectories in Fig. 1. The increase in the ratio of long jumps, which takes the form of a significant increase in the root-mean-square jump length $\langle l^2 \rangle^{1/2}$ in Fig. 1(b), which contrasts markedly with the weak temperature-dependence of the jump length in the usual activated surface diffusion.

Although longer-lived longer jumps have a tendency to have larger mean kinetic energy (mean velocity), μ' is always larger than μ . Probably, this is because, as shown in Fig. 1, jumps are not always ballistic (straight). Since each jump length l is defined as the distance between two consecutive sticking points, l can be much shorter than the corresponding actual migration length.

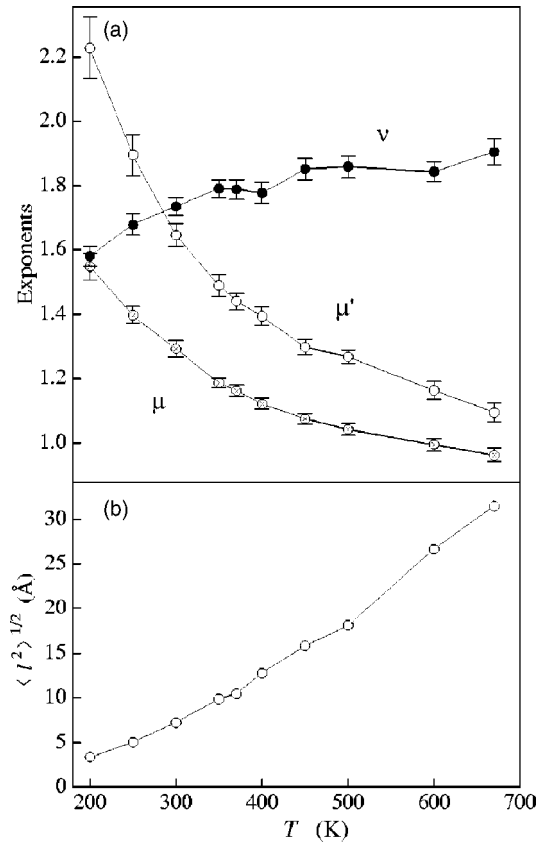


FIG. 3. Temperature dependence of (a) the power-law exponents [ν (sticking duration), μ (jump duration), and μ' (jump length)] and (b) the root-mean-square jump length $\langle l^2 \rangle^{1/2}$.

To clarify the temperature dependence of diffusivity, I measured diffusion coefficients from mean-square-displacements (MSD's) $\langle [\mathbf{R}(t+q) - \mathbf{R}(q)]^2 \rangle_q = \langle \Delta R^2(t) \rangle$ for x - y trajectories of $10 \mu\text{s}$, where $\langle * \rangle_q$ denotes a statistical average over the time q . Figure 4 shows (a) the log-log plots of MSD's and (b) their slopes, $\gamma(t) = d \log_{10} \langle \Delta R^2(t) \rangle / d \log_{10} t$. We can see from the figure that, for each temperature, diffusivity crosses over gradually from anomalous one ($\gamma > 1$) to normal one ($\gamma = 1$) at about a few ns. The superdiffusive behavior ($\gamma > 1$) for $t < \sim 10^3$ ps is due to the power-law correlated jump dynamics, which seemingly obeys a *genuine* Lévy-distribution having infinite variance.⁷ The damped oscillations of γ , which have an identical period of about 20 ps, are due to the oscillatory sticking motion within a potential,^{7,15} indicating the validity of the use of constant τ_c .

The inversion of the 300 and 400 K MSD curves and the increasing fluctuations in γ for $t > \sim 10^4$ ps are statistical errors due to a decrease in the number of samples for statistical averages over q with t . Hence we cannot use the conventional relation $D = \lim_{t \rightarrow \infty} \langle \Delta R^2(t) \rangle / 4t$. To measure long-time self-diffusion coefficients D , I therefore fit linear functions to the MSD's in the range of $10^3 < t < 10^4$ ps by using the least-squares method and divided the slopes by 4.

Figure 5 shows the Arrhenius plot of the diffusion coefficients in the broad range of 200–670 K. We can see from the figure that the diffusion coefficients are expressed, on a log scale, as a linear function of $1/k_B T$, clearly obeying an

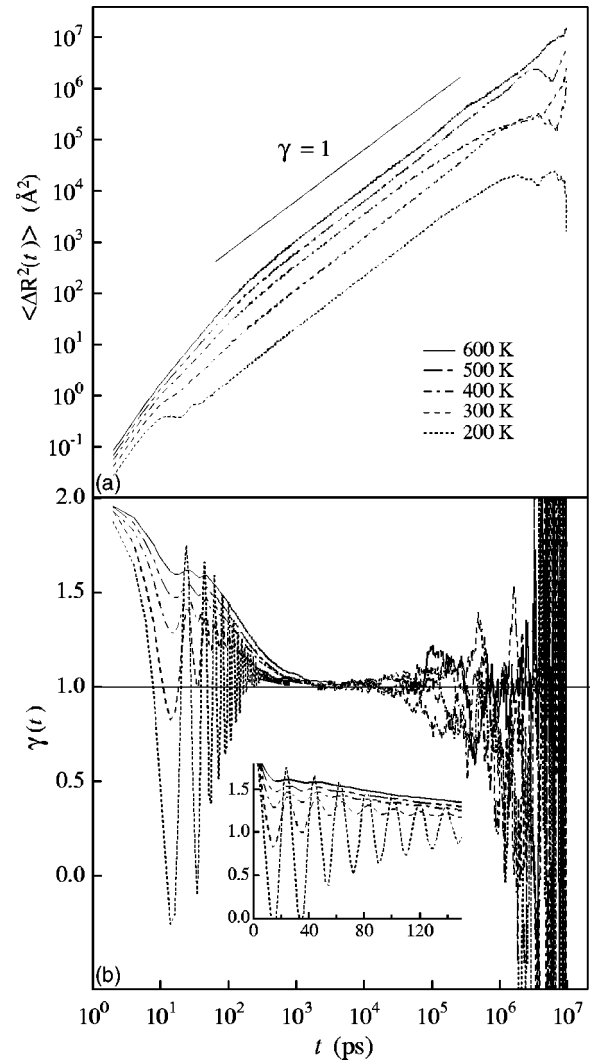


FIG. 4. (a) Log-log plots of MSD's [$\langle \Delta R^2(t) \rangle$] for 200, 300, 400, 500, and 600 K, and (b) their slopes $\gamma = d \log_{10} \langle \Delta R^2(t) \rangle / d \log_{10} t$. Inset: γ on a linear scale. The periodic oscillations are due to intra-well sticking motions, Ref. 15, having almost the same period of $\tau = 20$ ps.

Arrhenius law: $D = D_0 \exp(-E_a/k_B T)$ with $D_0 = 1.83 \times 10^{-4} \text{ cm}^2/\text{s}$, and $E_a = 0.103 \pm 0.003 \text{ eV}$.

Arrhenius diffusivity is generally believed to be due to activated jump diffusion dynamics; we therefore can conclude that the Lévy-type stick-slip diffusion is also an activated diffusion. Note, however, that the diffusion dynamics is far from the usual one. Long-lived long jumps as well as short stickings do not allow us to image a well-defined single activation-relaxation process such as adatom diffusion. The computed activation barrier E_a should be due to some complex average of various activation-relaxation processes, which is probably associated with rotational and many internal degrees of freedom, as depicted in Ref. 5.

The observation of Arrhenius temperature dependence is in itself consistent with the experimental results by Bardotti *et al.*¹ However, the Arrhenius parameters extracted in this work differ remarkably from the experimental ones:¹ $E_a = 0.5 \pm 0.1 \text{ eV}$ and $D_0 = 10^3 \text{ cm}^2/\text{s}$. In particular, the experi-

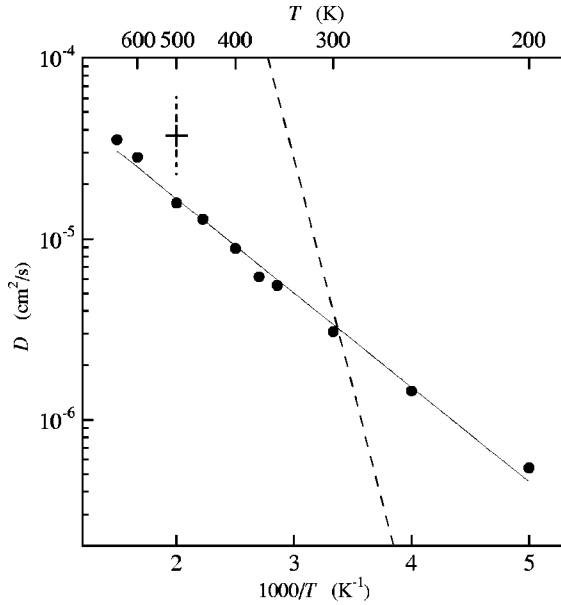


FIG. 5. Arrhenius plot of diffusion coefficients obtained from the MSD's in Fig. 4. Statistical uncertainty in the data is estimated to be smaller than the size of the dots. The solid line shows $D = D_0 \exp(-E_a/k_B T)$ with $D_0 = 1.83 \times 10^{-4} \text{ cm}^2/\text{s}$, and $E_a = 0.103 \text{ eV}$. The broken line represents the experimental result in Ref. 1: $D_0 = 10^3 \text{ cm}^2/\text{s}$, and $E_a = 0.5 \text{ eV}$. The plus represents a diffusion coefficient obtained with fully atomistic but short ($\sim 14 \text{ ns}$) MD simulations by Lewis *et al.* (Ref. 16).

mental diffusion prefactor D_0 is seven orders of magnitude larger than the computed one. The adoption of the simple model, which can cause discrepancies, does not allow us to compare the results directly to the experimental results. However, even when the largest possible tolerance is used, the huge discrepancy in D_0 is too large. Here I would like to comment on the large diffusion prefactor D_0 .

Experimentally, from measurements of saturation island densities, Bardotti *et al.*¹ found the mean diffusion time τ which is needed for a gold nanocluster to move in a random direction by one mean cluster diameter $d = 20 \text{ \AA}$, obtaining diffusion coefficients for various temperatures using the relation $D = d^2/4\tau$. Since d , adopted *a priori* as the minimum length scale in the model to analyze their experiments,¹ should be larger than the actual length scale of dominant motion responsible for the diffusion, τ should be larger than the actual time scale in which the dominant motion occurs. (If it is not so, one cannot obtain correct diffusion coefficients.) The actual time scale is deeply related to temperature (thermal velocity) as well as the length scale; hence τ should be larger than the thermally allowable lower bound. Contrary to this, one can find that, for $T > 340 \text{ K}$, τ becomes smaller than the lower bound. For example, for $T = 400 \text{ K}$, the Arrhenius parameters obtained experimentally give us $D \approx 5 \times 10^{-4} \text{ cm}^2/\text{s}$, and we obtain $\tau = d^2/4D \approx 20 \times 10^{-12} \text{ s} = 20 \text{ ps}$. This value of τ is far less than the time to cross over

d at thermal velocity, $\tau_{\text{th}} \sim d\sqrt{M/k_B T} = 240 \text{ ps}$ (M is the mass of Au_{250}), and unacceptable. It is unlikely that a cluster as a whole violates the law of energy equipartition. I consider that this is due to that the experimental D_0 is too large in value. (Generally, E_a affects only the temperature at which τ becomes smaller than the thermally allowable lower bound.)

The model used here, which seemingly lacks in quantitative prediction capability because of its simplicity, gives a result that is fairly consistent with the realistic MD simulations by Lewis *et al.*¹⁶ They performed fully atomistic MD simulations at 500 K by using many-body interatomic potentials (for Au–Au and C–C), obtaining $D = 3.71 \times 10^{-5} \text{ cm}^2/\text{s}$ [its statistical uncertainty was probably large because of short ($\sim 14 \text{ ns}$) MD runs]. This value approximately agrees with that computed in this work, $1.58 \times 10^{-5} \text{ cm}^2/\text{s}$, fairly well convincing us of the validity of the present MD simulations. The success of the present very simple model is presumably due to the applicability of so-called “adiabatic elimination” and the presence of power-law nature in the diffusion dynamics, as mentioned above.

IV. CONCLUSIONS

Long-lived long jumps as well as short stickings in the power-law correlated Lévy-type stick-slip diffusion⁵ imply that the cluster jumps without equilibrating locally with the surface, conflicting with the usual equilibrium Arrhenius jump rate processes. To clarify whether the diffusion exhibits Arrhenius diffusivity, I have computationally studied temperature dependence of the diffusion. To do this, I adopted a Langevin-thermostatted 2-D FK-type cluster-surface model to perform extremely long ($10 \mu\text{s}$) MD simulations for various temperatures. Here we found that diffusion coefficients computed from the MSD's obey an Arrhenius law: $D = D_0 \exp(-E_a/k_B T)$ with $D_0 = 1.83 \times 10^{-4} \text{ cm}^2/\text{s}$, and $E_a = 0.103 \text{ eV}$. On the other hand, we found that the power-law correlated stick-slip diffusion dynamics is in itself robust to temperature change, and that exponents that characterize the diffusion dynamics are not universal, but vary with temperature. The decrease in the jump length exponent represents a significant increase in the ratio of long jumps, contrasting to a weak temperature-dependence of jump length in the usual activated (Arrhenius-type) surface diffusion.

The results implies that Arrhenius diffusivity can be observed even if diffusion dynamics is far from the usual equilibrium Arrhenius jump rate processes. To further clarify the Arrhenius diffusivity in accord with the power-law correlated stick-slip diffusion dynamics, we need to investigate, for example, temperature-dependence of the mean stick-slip frequency and intra-well temperature of the cluster.

ACKNOWLEDGMENTS

I would like to acknowledge valuable discussions with J. Murakami, Y. Tai, and W. Yamaguchi.

- ¹L. Bardotti, P. Jensen, M. Treilleux, A. Hoareau, and B. Cabaud, *Surf. Sci.* **367**, 276 (1996), and references therein.
- ²S. C. Wang, U. Kurpick, and G. Ehrlich, *Phys. Rev. Lett.* **81**, 4923 (1998).
- ³M. Schunack, T. R. Linderth, F. Rosei, E. Laegsgaard, I. Stensgaard, and F. Besenbacher, *Phys. Rev. Lett.* **88**, 156102 (2002).
- ⁴J. Klafter, M. F. Shlesinger, and G. Zumofen, *Phys. Today* **49**, 33 (1996), and references therein.
- ⁵W. D. Luedtke and U. Landman, *Phys. Rev. Lett.* **82**, 3835 (1999).
- ⁶R. N. Mantegna and H. E. Stanley, *Phys. Rev. Lett.* **73**, 2946 (1994).
- ⁷Y. Maruyama and J. Murakami, *Phys. Rev. B* **67**, 085406 (2003).
- ⁸P. Hanggi, P. Talkner, and M. Borkovec, *Rev. Mod. Phys.* **62**, 251 (1990).
- ⁹The classical standard Frenkel–Kontorova model represents an infinitely long one-dimensional chain of particles harmonically coupled with their neighbors and subjected to an incommensurate sinusoidal potential.
- ¹⁰H. E. Stanley, *Introduction to Phase Transitions and Critical Phenomena* (Oxford University Press, Oxford, 1971).
- ¹¹P. Bak, C. Tang, and K. Wiesenfeld, *Phys. Rev. A* **38**, 364 (1988), and references therein.
- ¹²E. Ganz, K. Sattler, and J. Clarke, *Surf. Sci.* **219**, 33 (1989).
- ¹³M. P. Allen and D. J. Tildesley, *Computer Simulation of Liquids* (Oxford University Press, Oxford, 1987).
- ¹⁴V. P. Zhdanov, *Surf. Sci.* **214**, 289 (1989).
- ¹⁵R. Ferrando, R. Spadacini, G. E. Tommei, and G. Caratti, *Surf. Sci.* **311**, 411 (1994).
- ¹⁶L. J. Lewis, P. Jensen, N. Combe, and J-L. Barrat, *Phys. Rev. B* **61**, 16 084 (2000).